

# A Mechanistic Understanding of Pronoun Fidelity in LLMs

Katharina Trinley<sup>1</sup> Jesujoba O. Alabi<sup>1</sup> Dietrich Klakow<sup>1</sup> Vagrant Gautam<sup>2</sup>

<sup>1</sup>Saarland University, Germany

<sup>2</sup>Heidelberg Institute for Theoretical Studies, Germany

katharinatrinley@icloud.com

## Abstract

Faithful and robust pronoun use is important for fair and coherent generations, yet large language models largely fail when multiple referents use different pronouns. To study the interplay of reasoning, repetition, and bias in this task, prior work relies exclusively on behavioural approaches, which may not reflect a model’s internal workings. Therefore, we provide a mechanistic, model-internal perspective on pronoun fidelity, testing whether three mechanisms—group entity binding ( $\mathcal{G}$ ), recency bias ( $\mathcal{R}$ ), and stereotypical bias ( $\mathcal{S}$ )—are causally implemented across several SOTA language models. Using Boundless Distributed Alignment Search, we find all three coexist as causal subspaces distributed across network depth. No single mechanism fully explains model behaviour, but a combination of the three consistently accounts for 91-99.5%. An attention head analysis further reveals two competing copying routes; group binding and stereotype share a localized concept-level route that retrieves a bound occupation-pronoun unit, while recency uses a distributed token-level route that repeats surface forms. In sum, pronoun fidelity arises from competition between simultaneously active causal subspaces.<sup>1</sup>

## 1 Introduction

Large language models (LLMs) demonstrate impressive performance across a range of NLP tasks and capabilities, including natural language understanding, various forms of reasoning (Guo et al., 2025), and in-context learning (Brown et al., 2020). Yet *why* they make the predictions they do remains largely unknown (Ferrando et al., 2024; Sharkey et al., 2025). While we understand their low-level mathematical operations and can observe their high-level input-output behaviour, the internal

<sup>1</sup>We release code at <https://github.com/KatharinaTrinley/pronoun-fidelity-mechanisms>.

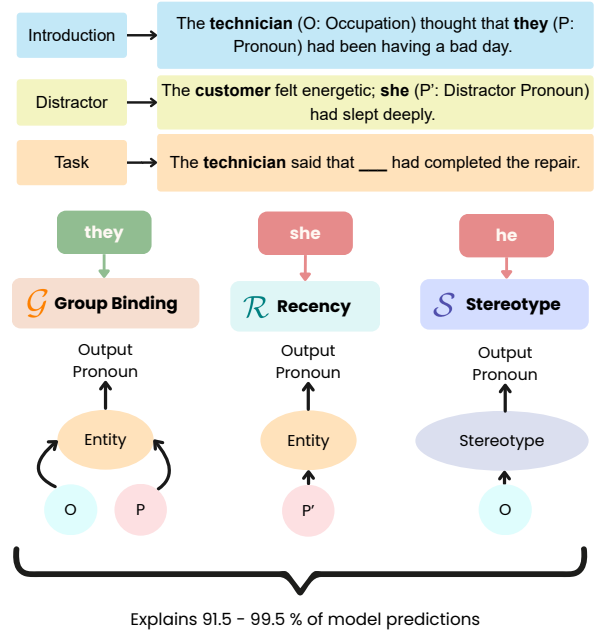


Figure 1: Pronoun fidelity task where model behaviour corresponds to three mechanistic hypotheses:  $\mathcal{G}$  **Group Binding Mechanism**: Occupation and explicit pronoun jointly determine correct entity-pronoun binding.  $\mathcal{R}$  **Recency Bias Mechanism**: Most recent pronoun mention determines output, overriding correct binding.  $\mathcal{S}$  **Stereotype Mechanism**: Occupation determines stereotypical pronoun association, ignoring context.

computational mechanisms that connect the two are opaque (Alishahi et al., 2019; Geiger et al., 2025). Consider a model that consistently predicts *he* when asked to generate a pronoun for a technician, even when the surrounding context provides evidence that *they* should be used. Understanding whether this prediction arises due to a stereotypical gendered association for the occupation requires more than behavioural evaluation; it requires looking inside the model for a faithful, causal account of its mechanisms (Geiger et al., 2025).

One area with great potential for causal analysis is pronoun fidelity, i.e., faithfully reusing pronouns for a referent regardless of intervening referents

who use different pronouns (see Figure 1). Introduced in Gautam et al. (2024), this is a task that is trivial for humans, yet challenging for state-of-the-art models (Subramonian et al., 2025; Gautam, 2026), where pronominal reasoning competes with shallow heuristics such as stereotypical biases and repetition of the most recent pronoun. As these mechanisms are only analyzed behaviourally in prior work, we contribute the *first mechanistic interpretability study of pronoun fidelity*.

Our analysis uses two complementary approaches: First, via Distributed Alignment Search, we show that the three mechanisms for pronoun fidelity coexist as separable causal subspaces. Although no single one dominates, they can be combined into a mixture model that predicts 91-99.5% of model behaviour. Second, an attention head analysis shows that pronoun information reaches the answer position via two competing copying routes. One copies the occupation-pronoun pair as a semantic unit, the other copies the surface form. Overall, our analyses reveal that pronoun fidelity emerges from a complex competition between multiple, simultaneously active causal subspaces.

## 2 Background

### 2.1 Pronoun Fidelity

The pronoun fidelity task, introduced in Gautam et al. (2024), is intuitively simple: Given a context that introduces an entity with an explicit pronoun (e.g., “The technician thought that he had been having a bad day”), the model must use that same pronoun when referring to the entity later (“The technician said that \_\_\_ had completed the repair”). The authors propose RUFF, a dataset of over 5 million instances designed to evaluate this task. Even in this minimal setting, models show systematic performance discrepancies. Accuracy is highest for *he/him/his* and degrades progressively for *she/her/hers*, singular *they/them/their*, and the neopronoun set *xe/xem/xyr*.

Performance degrades further as discourse complexity increases. Adding just a single sentence about a different entity (e.g., “The customer felt energetic; she had slept deeply.”) causes accuracy to drop by 34% (Gautam et al. (2024), Appendix E), in a setting where humans make virtually no errors. This motivates the question: *Are language models reasoning about pronouns, repeating surface patterns, or relying on statistical gender biases?* Gautam et al. (2024) attempt to

answer this by examining model behaviour; we instead consider model-internal mechanisms.

### 2.2 Distributed Alignment Search

To recover the pronoun fidelity mechanisms causally rather than behaviourally, we use Distributed Alignment Search (DAS). DAS (Geiger et al., 2024) learns an orthogonal rotation matrix  $R \in \mathbb{R}^{d \times d}$  over the residual stream  $\mathbf{h} \in \mathbb{R}^d$ , finding the directions in which a high-level target concept is linearly encoded. A distributed interchange intervention then swaps  $k$  dimensions from a source input  $s$  into a base input  $b$  in the rotated space and rotates back:

$$F_N^*(b) = R^{-1} \left( \text{Proj}_{Y_0}(R(F_N(b))) + \sum_{j=1}^k \text{Proj}_{Y_j}(R(F_N(s_j))) \right), \quad (1)$$

where  $Y_0, Y_1, \dots, Y_k$  form an orthogonal decomposition of  $\mathbb{R}^d$ ,  $Y_0$  preserves information from the base input, and  $Y_1, \dots, Y_k$  inject information from the source inputs  $s_j$ . Intuitively, DAS searches for a subspace that causally carries the target concept by checking whether transplanting a subspace from one input to another changes the output.

Standard DAS requires a manual search over the subspace dimensionality  $k$ . Boundless DAS (Wu et al., 2023) instead makes  $k$  learnable through differentiable soft boundaries. With boundary scalars  $c_j$  and a temperature  $\beta$ , the sigmoid function  $\sigma$  and index  $i$  over the rotated dimensions:

$$(M_j)_k = \sigma \left( \frac{i - c_j}{\beta} \right) \cdot \sigma \left( \frac{c_{j+1} - i}{\beta} \right), \quad (2)$$

As  $\beta$  is annealed toward zero during training, the masks converge to binary vectors, jointly optimizing  $R$  and the subspace size.

With **Interchange Intervention Accuracy** (IIA), we measure the fraction of cases where the intervened network’s output matches the high-level prediction; high IIA means the causal hypothesis is faithfully implemented. Each intervention uses two counterfactual inputs: we run and modify the *base*, injecting information read from the *source*.

## 3 Experimental Setup

Our evaluation spans ten model variants (§3.1). We consider three mechanistic hypotheses (§3.2, build diagnostic datasets from RUFF to isolate them (§3.3), and use these to train boundless DAS (§3.4).

Dataset	Base - Example	Source - Example
GR Dataset (isolates $\mathcal{S}$ as $\mathcal{G}_{source} = \mathcal{R}_{source}$ )	“The <i>technician</i> (stereotype: <i>he</i> ) thought that <i>they</i> had been having a bad day. The customer felt energetic; <i>she</i> had slept deeply. The technician said that ___ had completed the repair.” [ $\mathcal{G}$ : <i>they</i> ]; [ $\mathcal{R}$ : <i>she</i> ]; [ $\mathcal{S}$ : <i>he</i> ]	“The <i>technician</i> (stereotype: <i>he</i> ) thought that <i>she</i> had been having a bad day. The technician said that ___ had completed the repair.” [ $\mathcal{G}$ : <i>she</i> ]; [ $\mathcal{R}$ : <i>she</i> ]; [ $\mathcal{S}$ : <i>he</i> ]
GS Dataset (isolates $\mathcal{R}$ as $\mathcal{G}_{source} = \mathcal{S}_{source}$ )	“The <i>technician</i> (stereotype: <i>he</i> ) thought that <i>they</i> had been having a bad day. The customer felt energetic; <i>she</i> had slept deeply. The technician said that ___ had completed the repair.” [ $\mathcal{G}$ : <i>they</i> ]; [ $\mathcal{R}$ : <i>she</i> ]; [ $\mathcal{S}$ : <i>he</i> ]	“The <i>technician</i> (stereotype: <i>he</i> ) thought that <i>he</i> had been having a bad day. The technician said that ___ had completed the repair.” [ $\mathcal{G}$ : <i>he</i> ]; [ $\mathcal{R}$ : <i>she</i> ]; [ $\mathcal{S}$ : <i>he</i> ]
RS Dataset (isolates $\mathcal{G}$ as $\mathcal{R}_{source} = \mathcal{S}_{source}$ )	“The <i>technician</i> (stereotype: <i>he</i> ) thought that <i>they</i> had been having a bad day. The customer felt energetic; <i>he</i> had slept deeply. The technician said that ___ had completed the repair.” [ $\mathcal{G}$ : <i>they</i> ]; [ $\mathcal{R}$ : <i>he</i> ]; [ $\mathcal{S}$ : <i>he</i> ]	“The <i>technician</i> (stereotype: <i>he</i> ) thought that <i>she</i> had been having a bad day. The technician said that ___ had completed the repair.” [ $\mathcal{G}$ : <i>she</i> ]; [ $\mathcal{R}$ : <i>he</i> ]; [ $\mathcal{S}$ : <i>he</i> ]

Table 1: Diagnostic datasets (each  $N = 14,400$ ) based on RUFF, designed to isolate the mechanisms we test.

### 3.1 Models

We experiment with ten decoder-only, instruction tuned models of varying sizes from four families. From the Llama-3.1 family (Grattafiori et al., 2024) we use LLAMA-3.1-8B-INSTRUCT and LLAMA-3.1-70B-INSTRUCT; from Gemma-2 (Team et al., 2024), GEMMA-2-9B-IT and GEMMA-2-27B-IT; from Qwen2.5 (Yang et al., 2025), QWEN2.5-7B-INSTRUCT and QWEN2.5-72B-INSTRUCT; and from OLMo-2 (Walsh et al., 2025), OLMo-2-0425-1B-INSTRUCT, OLMo-2-1124-7B-INSTRUCT, OLMo-2-1124-13B-INSTRUCT, and OLMo-2-0325-32B-INSTRUCT.

We score model responses by comparing log-probabilities of just the pronoun options (*he*, *she*, *they*, and inflections), in a carrier prompt (see Appendix B) following Gautam et al. (2024). This is necessary as sometimes tokens like “*the*” can have higher probability than a pronoun.

### 3.2 Candidate Mechanisms

We consider three candidate mechanisms, reformulating Gautam et al. (2024)’s hypotheses about model *behaviour* as *mechanistic* hypotheses, i.e., causal models that explain how internal representations might drive predictions.

**Mechanism  $\mathcal{G}$ : Group Entity.** Models may resolve pronouns by retrieving a single bound group entity that jointly encodes the occupation noun and its explicitly stated pronoun (Prakash et al., 2024). Under this mechanism, querying “*technician*” retrieves the complete group  $\langle \text{technician, they} \rangle$ , and the correct pronoun is read off directly. This is in some sense the desired behaviour as it grounds the prediction in the context and remains robust to

distractors. However, the binding is formed from surface co-occurrence in the introduction sentence and could be broken by more adversarial contexts.

**Mechanism  $\mathcal{S}$ : Stereotype Bias.** Models may use associations between occupations and gendered pronouns learned from patterns in pre-training data (Gallegos et al., 2024), rather than the context. When maintaining entity-pronoun bindings becomes demanding, these stereotypical associations may serve as a convenient fallback.

**Mechanism  $\mathcal{R}$ : Recency Bias.** Under discourse complexity, accurate entity-pronoun bindings may be overridden by a preference for the most recently mentioned pronoun, leading to errors.

Note that both  $\mathcal{G}$  and  $\mathcal{S}$  tie a pronoun to the occupation (but based on different information: Context vs. stereotypical bias), while  $\mathcal{R}$  tracks only surface position. We return to this distinction in §6.

### 3.3 Data

We create three diagnostic datasets to test whether our candidate mechanisms are causally separable. All of these are based on RUFF (see §2.1). Each example consists of an introductory sentence (which contains the target entity and pronoun), 0-5 distractor sentences about a different participant with a different pronoun, and a task sentence in which the model must fill in the blank to refer to the target entity again with the correct target pronoun. We focus on three pronoun sets (*he/him/his*, *she/her/her*, singular *they/them/their*), and exclude the neopronoun set *xe/xem/xyr* from our analysis, as neopronouns are too sparsely represented in training data and are thus rarely tokenized singly (Ovalle et al., 2024).

As Table 1 shows, each diagnostic dataset ( $N = 14,400$  instances) is designed such that two mechanisms agree on a pronoun prediction in the source, allowing us to isolate the third mechanism.

### 3.4 Training DAS Models

For a given model layer, we train three boundless DAS featurizers per mechanism and dataset. As different mechanisms may be encoded at different network depths, we train at every second layer across models, and select the one with the highest IIA on the evaluation set separately for each mechanism and language model, following Wu et al. (2023). For mechanism  $\mathcal{S}$  we use a stereotype-specific variant  $IIA_{\text{stereotype}}$  that checks whether the post-intervention prediction matches the stereotypical pronoun for the source occupation rather than the source sentence’s explicit pronoun. Further details are provided in Appendix D.

## 4 DAS Recovers Three Subspaces

We use boundless DAS to test whether the three hypothesized mechanisms are causally implemented. First, we do a layer search to locate each mechanism (§4.1). Then, we train fully on all diagnostic datasets (§4.2). Finally, we experiment with cross-mechanism transfer to evaluate whether the subspaces we recover are distinct (§4.3).

### 4.1 Layer Search

Since DAS intervenes on a single layer at a time, and different causal mechanisms may be encoded at different network depths, we search for the layer at which each mechanism is most strongly represented. Table 2 reports the best layer and corresponding IIA for each model and mechanism (full layer search results are shown in Appendix F). We find that *every mechanism is recoverable somewhere in the network*; no hypothesis can be ruled out on the grounds that its subspace does not exist.

#### Different mechanisms dominate per model.

Which mechanism is most recoverable, however, varies by model, and no single mechanism dominates.  $\mathcal{G}$  and  $\mathcal{R}$  generally reach higher IIA than  $\mathcal{S}$ : In Llama-3.1-8B, OLMo-2-1B, and Gemma-2-9B all three reach 0.78, 0.78, and 1.0, against 0.74, 0.60, and 0.90 for  $\mathcal{S}$  and in OLMo-2-7B  $\mathcal{G}$  reaches 0.935 versus 0.665 for  $\mathcal{S}$ . The ordering is not universal, though, as in Qwen2.5-7B and OLMo-2-13B  $\mathcal{S}$  leads instead (0.84 and 0.76), ahead of  $\mathcal{R}$  (0.76, 0.72) and  $\mathcal{G}$  (0.74, 0.62).

Model	Mechanism	$\ell_{best}$	$IIA_{Best}$
Llama-8B	Group Binding $\mathcal{G}$	8	<b>0.78</b>
	Stereotype $\mathcal{S}$	8	0.74
	Recency $\mathcal{R}$	8	<b>0.78</b>
OLMo-1B	Group Binding $\mathcal{G}$	12	<b>0.78</b>
	Stereotype $\mathcal{S}$	2	0.60
	Recency $\mathcal{R}$	6	<b>0.78</b>
OLMo-7B	Group Binding $\mathcal{G}$	14	<b>0.94</b>
	Stereotype $\mathcal{S}$	14	0.67
	Recency $\mathcal{R}$	16	0.64
OLMo-13B	Group Binding $\mathcal{G}$	10	0.62
	Stereotype $\mathcal{S}$	10	<b>0.76</b>
	Recency $\mathcal{R}$	5	0.72
Gemma-9B	Group Binding $\mathcal{G}$	10	<b>1.00</b>
	Stereotype $\mathcal{S}$	15	0.90
	Recency $\mathcal{R}$	10	<b>1.00</b>
Qwen-7B	Group Binding $\mathcal{G}$	14	0.74
	Stereotype $\mathcal{S}$	7	<b>0.84</b>
	Recency $\mathcal{R}$	14	0.76

Table 2: Best layer and IIA per model and mechanism.

**The mechanisms sit at different depths.** Within a single model the best layer usually differs across mechanisms; in OLMo-2-7B, for instance,  $\mathcal{G}$  sits at layer 8,  $\mathcal{R}$  at layer 6, and  $\mathcal{S}$  at layer 0. This is a first indication that we are recovering three separate subspaces rather than one shared representation. However, this evidence is only suggestive; since IIA here is measured on the mixed dataset, two mechanisms can score similarly high simply because they happen to agree on a prediction. We disentangle this in the experiments that follow.

### 4.2 Full Training

Having located each mechanism, we now train DAS at the selected layers on the full diagnostic datasets, each of which isolates one mechanism by construction (see §3.3). Table 3 reports the results.

#### All three mechanisms remain causally active.

In most cases, the mechanism that scores highest in the layer search remains strong across the three diagnostic datasets, though this is not consistent for every model.  $\mathcal{S}$  is the strongest mechanism for Qwen2.5-7B as before, and now also for Gemma2-9B, despite having been its weakest mechanism during layer search. For Llama, OLMo-1B, OLMo-7B the dominant mechanism also carries over, with  $\mathcal{R}$  performing best on GR and GS whereas  $\mathcal{G}$  dominates on the RS dataset. Across all datasets, no single mechanism dominates, and the IIAs are broadly comparable. This reinforces the idea that pronoun fidelity is not a single-mechanism problem.

Dataset	Mechanism	Llama-8B	OLMo-1B	OLMo-7B	OLMo-13B	Gemma-9B	Qwen-7B
GR (isolates $\mathcal{S}$ )	Group Binding $\mathcal{G}$	0.59	0.25	0.49	0.66	0.60	0.92
	Stereotype $\mathcal{S}$	0.58	0.38	<b>0.69</b>	<b>0.89</b>	0.60	<b>0.95</b>
	Recency $\mathcal{R}$	<b>0.68</b>	<b>0.85</b>	0.60	0.735	<b>1.00</b>	0.82
GS (isolates $\mathcal{R}$ )	Group Binding $\mathcal{G}$	0.58	0.40	0.56	0.89	0.55	0.96
	Stereotype $\mathcal{S}$	0.59	0.47	0.69	<b>0.89</b>	0.68	<b>0.97</b>
	Recency $\mathcal{R}$	<b>0.80</b>	<b>0.89</b>	<b>0.84</b>	0.78	<b>0.70</b>	0.87
RS (isolates $\mathcal{G}$ )	Group Binding $\mathcal{G}$	<b>0.75</b>	<b>0.79</b>	<b>0.75</b>	0.76	0.52	0.93
	Stereotype $\mathcal{S}$	0.71	0.56	0.53	<b>0.77</b>	<b>0.55</b>	<b>1.00</b>
	Recency $\mathcal{R}$	0.69	0.59	0.74	0.63	<b>0.55</b>	0.95

Table 3: Best IIA per mechanism and dataset across models after full training on the diagnostic datasets.

Model	Rotation matrix $\mathbf{R}$	GS	RS	GR
Llama-8B	$\mathcal{G}$ ( $\ell = 8$ )	0.55	0.55	<b>0.65</b>
	$\mathcal{S}$ ( $\ell = 8$ )	0.59	<b>0.60</b>	0.60
	$\mathcal{R}$ ( $\ell = 8$ )	<b>0.68</b>	0.49	0.32
OLMo-1B	$\mathcal{G}$ ( $\ell = 12$ )	0.47	0.36	0.33
	$\mathcal{S}$ ( $\ell = 6$ )	0.63	0.50	<b>0.40</b>
	$\mathcal{R}$ ( $\ell = 2$ )	<b>0.89</b>	<b>0.83</b>	0.13
OLMo-7B	$\mathcal{G}$ ( $\ell = 8$ )	0.35	0.30	<b>0.63</b>
	$\mathcal{S}$ ( $\ell = 6$ )	0.34	0.33	0.68
	$\mathcal{R}$ ( $\ell = 0$ )	<b>0.74</b>	<b>0.53</b>	0.57
OLMo-13B	$\mathcal{G}$ ( $\ell = 10$ )	0.54	0.56	0.80
	$\mathcal{S}$ ( $\ell = 10$ )	0.54	0.61	<b>0.82</b>
	$\mathcal{R}$ ( $\ell = 0$ )	<b>0.73</b>	<b>0.75</b>	0.58
Gemma-9B	$\mathcal{G}$ ( $\ell = 10$ )	0.26	0.51	0.44
	$\mathcal{S}$ ( $\ell = 10$ )	0.14	<b>0.70</b>	<b>0.70</b>
	$\mathcal{R}$ ( $\ell = 10$ )	<b>0.99</b>	0.12	0.00
Qwen-7B	$\mathcal{G}$ ( $\ell = 14$ )	0.32	0.34	<b>0.94</b>
	$\mathcal{S}$ ( $\ell = 7$ )	0.39	0.37	0.81
	$\mathcal{R}$ ( $\ell = 14$ )	<b>0.90</b>	<b>0.78</b>	0.53

Table 4: Cross-mechanism specificity per model. Rows index the trained rotation matrix and columns the diagnostic dataset. The best rotation per dataset is **bolded**.  $\mathcal{G}$  and  $\mathcal{S}$  tend to peak together on GR in most models, while  $\mathcal{R}$  peaks on GS, showing that  $\mathcal{G}$  and  $\mathcal{S}$  behave alike while  $\mathcal{R}$  is distinct.

### 4.3 Validation

The layer search and full training establish that each mechanism is individually sufficient to flip a prediction, but not that the three subspaces are genuinely distinct. We test specificity using the structure of the diagnostic datasets (§3.3), since each isolates one mechanism. We take the three rotation matrices  $R_G$ ,  $R_R$ ,  $R_S$ , freeze them, and evaluate each on every dataset, giving a  $3 \times 3$  matrix per model (rotation  $\times$  evaluation dataset; Table 4).

**Recency is distinct; group binding and stereotype overlap.** Across all models,  $\mathcal{R}$  is the most distinct rotation: It dominates GS and transfers beyond this to RS as well. With GR, in contrast, either

$\mathcal{G}$  or  $\mathcal{S}$  wins, and the two are never clearly distinct from each other on any dataset. In general, the  $\mathcal{G}$  and  $\mathcal{S}$  rotations tend to score similarly high or similarly low on the same datasets, whereas  $\mathcal{R}$  scores high exactly where the others score low, and vice versa.  $\mathcal{G}$  and  $\mathcal{S}$  thus behave as one overlapping subspace, while  $\mathcal{R}$  stays separable.

**Takeaway.** We recover three causal subspaces for pronoun fidelity, each of which is sufficient to flip predictions, without a single mechanism dominating. Cross-mechanism transfer shows that  $\mathcal{G}$  and  $\mathcal{S}$  behave similarly, while  $\mathcal{R}$  stays distinct.

## 5 A Mixture of Mechanisms Explains Model Behaviour

If no single mechanism dominates, *how do the three combine to produce model behaviour?* Following the causal model combination approach of Pflsar et al. (2025) and Gur-Arieh et al. (2026), we fit a lightweight mixture model on the mechanisms.

**Fitting the mixture model.** For each mechanism we collect empirical next-token distributions over {he, she, they} via inference-only interchange interventions: We patch the source residual stream into the base run at the best layer  $\ell$  identified in our DAS layer search (§4.1), with no trained rotation, and read off the softmax over the three pronouns. For larger models where a full DAS training layer search is computationally infeasible (32B–72B), we instead identify  $\ell$  with an inference-only search over a 200-example subset of the mixed datasets, applying VanillaIntervention patches (Wu et al., 2024) that overwrite the base residual stream with the source vector. We select the last layer at which the base pronoun still dominates, i.e., the point just before the intervention takes effect and the model commits to an answer.

Each softmax distribution is indexed at the re-

Model	$\ell_G/\ell_R/\ell_S$	$\mathcal{M}$	$\mathcal{M}\setminus\{G\}$	$\mathcal{M}\setminus\{R\}$	$\mathcal{M}\setminus\{S\}$	$\mathcal{M}\setminus\{G, R\}$	$\mathcal{M}\setminus\{G, S\}$	$\mathcal{M}\setminus\{R, S\}$
Llama-8B	8/8/8	0.970	<b>0.974</b>	0.972	0.967	0.932	0.966	0.949
Llama-70B	48/0/48	<b>0.943</b>	0.934	0.920	0.936	0.919	0.918	0.889
OLMo-1B	12/2/6	<b>0.995</b>	0.994	0.991	0.983	0.991	0.960	0.908
OLMo-7B	14/14/16	<b>0.961</b>	<b>0.961</b>	0.943	0.945	0.943	0.943	0.884
OLMo-13B	10/10/5	0.953	<b>0.975</b>	0.928	0.931	0.928	0.946	<b>0.959</b>
OLMo-32B	60/60/60	<b>0.991</b>	0.987	0.988	0.987	0.984	0.985	0.980
Gemma-9B	10/15/10	<b>0.958</b>	0.957	0.947	0.935	0.946	0.933	0.874
Gemma-27B	40/40/0	<b>0.976</b>	0.952	0.962	0.954	0.915	0.926	0.898
Qwen-7B	14/7/14	<b>0.915</b>	<b>0.915</b>	0.871	0.859	0.870	0.856	0.700
Qwen-72B	48/0/0	<b>0.964</b>	0.962	0.947	0.936	0.947	0.935	0.864

Table 5: Jensen-Shannon similarity between predicted and empirical pronoun distributions for the full mixture model  $\mathcal{M}$  and selected ablations. Higher is better. The best value in each row is shown in bold; the lowest value is shown in gray.  $\ell_G$ ,  $\ell_R$ , and  $\ell_S$  denote the layer selected for each mechanism.

sponse position by the triple  $(g, r, s)$ : The pronouns predicted by group binding, recency, and stereotype, respectively. The mixture model predicts:

$$\begin{aligned} \text{logit}(a) = & w_G \cdot \mathbf{1}\{a = g\} \\ & + w_R[r] \cdot \mathbf{1}\{a = r\} \\ & + w_S[s] \cdot \mathbf{1}\{a = s\}, \end{aligned} \quad (3)$$

where  $a \in \{he, she, they\}$ . The scalar  $w_G$  and the pronoun-indexed vectors  $w_R[\cdot]$  and  $w_S[\cdot]$  are trained with Adam (learning rate 0.05) and a Jensen-Shannon divergence loss. We report Jensen-Shannon similarities ( $JSS \in [0, 1]$ ,  $1 - JSD$ ) in Table 5 for the mixture model  $\mathcal{M}$  and all single- and double-mechanism ablations. Higher values show agreement between the mixture model’s prediction and the empirical distribution of model behaviour. The full model consistently achieves high JSS (0.915–0.995), indicating that the three mechanisms together account for almost all behaviour.

**Recency and stereotype carry most of the signal.** Ablations where recency and stereotype are jointly removed ( $\mathcal{M}\setminus\{R, S\}$ ) causes JSS to drop the most across nearly all models, while removing either alone causes smaller but consistent degradation. We can thus conclude that model behaviour relies primarily on these two heuristics.

**Group binding contributes little.** Removing group binding ( $\mathcal{M}\setminus\{G\}$ ) sometimes leaves JSS unchanged, or even improves it, matching or exceeding the full model across several models (by 0.022 in OLMo-13B). Rather than adding a signal beyond what the recency and stereotype mechanisms already capture, *group binding can add noise*.

These patterns even line up somewhat with model-specific DAS results from §4: In Qwen-7B, where  $S$  is the dominant subspace, ablating

$\mathcal{M}\setminus\{S\}$  hurts JSS, dropping from 0.915 to 0.859; in OLMo-13B, where  $G$  achieves lowest IIA, removing it from the mixture model actually helps.

**Takeaway.** Pronoun fidelity can be fully explained by a combination of mechanisms: Recency and stereotype carry most of the signal, while group binding contributes little and can even add noise.

## 6 Attention Head Analysis

So far we have shown which mechanisms are at play in pronoun fidelity, where they are located, and how they combine, but not which components of a model *implement* them. Inspired by Feucht et al. (2025), we look at individual attention heads.

Feucht et al. (2025) find that LLMs use attention heads to implement two parallel copying routes: *Token-level induction heads* match exact individual subword tokens, while *concept-level induction heads* attend to the ends of multi-token words and copy full words as abstract concepts for tasks like translations and paraphrasing. In our setting, we posit that concept-level copying corresponds to retrieving a bound semantic unit (the occupation-pronoun pair) which is what both group binding  $G$  and stereotype bias  $S$  rely on. Token-level copying corresponds to recency  $R$ , where the model repeats the most recent pronoun. To test whether concept-level or token-level copying dominates pronoun fidelity, we identify and ablate the attention heads responsible for each copying route.

**Identification.** We identify attention heads responsible for a particular copying route by patching pre-projection outputs from clean to corrupt instances of two new datasets that isolate concept-level and token-level copying (see Table 6). If the head carries information about the occupation-pronoun group as a concept, then it will ignore

Dataset	Clean - Example	Corrupt - Example
concept-level (pron: <i>he</i> )	The technician thought that <i>he</i> had been having a bad day. The customer felt energetic; <i>she</i> had slept deeply. The technician said that ___ had completed the repair.	The customer felt energetic; <i>she</i> had slept deeply. The technician thought that <i>he</i> had been having a bad day. The technician said that ___ had completed the repair.
token-level (pron: <i>she</i> )	The customer felt energetic; <i>she</i> had slept deeply. The technician thought that <i>he</i> had been having a bad day. The technician said that ___ had completed the repair.	The technician thought that <i>he</i> had been having a bad day. The customer felt energetic; <i>she</i> had slept deeply. The technician said that ___ had completed the repair.

Table 6: Examples from the two copying datasets. Each dataset contains 50 data points to identify the heads and 50 data points on which we ablate. Clean activations are patched into the corrupt run.

Model	Heads	$\Delta A(A_{abl} - A_{base})$	$\Delta A_{rd}$
concept-level			
Llama-8B	11	-0.04 (0.96 - 1.00)	-0.04
OLMo-1B	11	-0.78 (0.16 - 0.94)	-0.07
OLMo-7B	11	-0.64 (0.16 - 0.80)	0.00
OLMo-13B	16	-0.28 (0.70 - 0.98)	0.00
Gemma-9B	23	-0.12 (0.86 - 0.98)	-0.02
Qwen-7B	29	-0.58 (0.30 - 0.88)	-0.07
token-level			
Llama-8B	21	+0.40 (0.76 - 0.48)	-0.04
OLMo-1B	72	-0.36 (0.44 - 0.80)	-0.22
OLMo-7B	41	-0.36 (0.08 - 0.34)	-0.01
OLMo-13B	61	-0.04 (0.64 - 0.68)	0.00
Gemma-9B	49	-0.16 (0.64 - 0.80)	-0.03
Qwen-7B	1	+0.44 (0.90 - 0.46)	-0.05

Table 7: Accuracy with cumulative head ablations for concept-level and token-level copying.  $A_{base}/A_{abl}$  denote base and ablated accuracy;  $A_{rd}$  shows accuracy when ablating the same number of heads at random.

recency information and consistently predict *he* on clean and corrupt instances of the concept-level dataset. In contrast, the token-level dataset tests whether the head directly copies the last seen pronoun token (e.g., copying *he* in the clean version and *she* in the corrupt version of the example).

For each attention head  $a^{(l,h)}$ , we patch its pre-projection output at the final token position from the clean run into the corrupt run, and measure

$$\Delta_{\log P}^{(l,h)} = \log P_{\text{patched}}(\text{pron}) - \log P_{\text{corrupt}}(\text{pron}),$$

where “pron” is the target entity’s pronoun in the concept copying experiment, and the distractor pronoun in the token-level experiment. Heads with high  $\Delta_{\log P}^{(l,h)}$  in the concept copying dataset are concept induction heads; heads with high  $\Delta_{\log P}^{(l,h)}$  on the token-level dataset implement token-level copying.

**Ablation.** We ablate heads by zeroing out the pre-projection  $a^{(l,h)}$  of each top-k (k=100) head at the final token position of the clean prompt. We then

measure the drop in  $\log P(\text{pron})$ :

$$\Delta_{\text{ablate}}^{(l,h)} = \log P_{\text{ablated}}(\text{pron}) - \log P_{\text{clean}}(\text{pron}).$$

We perform *single head ablations* with one top-k head zeroed out at a time, and *cumulative ablations*, where heads are zeroed in rank order. Both use  $N = 50$  held-out examples not seen during identification, scored by log probabilities.

**Results.** We show accuracy drops with cumulative head ablation in Table 7. Further results are shown in Appendix G. For **concept-level copying**, a small set of heads have substantial causal effects: Removing identified heads causes large, consistent accuracy drops. OLMo-1B and OLMo-7B both fall to 0.16 after ablating only 11 heads; Qwen-7B drops to 0.30 after 29. A random ablation baseline, removing the same number of heads at random, has almost no effect, confirming the drop is specific to the identified heads. This provides evidence of a localizable concept-copying route. Llama-3.1-8B is the exception: its targeted drop matches its random baseline, consistent with its flat causal scores and a more distributed concept route.

For **token-level copying**, there is no distinct set of high-scoring heads, suggesting the mechanism is distributed across many heads. Many heads must be ablated for accuracy to change, e.g., OLMo-2-1B degrades from 0.80 to 0.44 only after ablating 72 heads, and OLMo-13B is almost unaffected after ablating 61 heads. Interestingly, for Qwen-7B and Llama-8B, ablating the identified token-copying heads does not lower accuracy but *raises* it (+0.44 and +0.40). This indicates competition between the two copying routes during pronoun resolution under discourse complexity.

**Takeaway.** Pronoun fidelity is solved via two competing copying routes that are localized differently: Concept copying through a few heads, and

token copying distributed across many low-effect heads. They compete, as evidenced by ablating token copying heads flipping a model from recency-driven bias to correct resolution, but which route dominates is model-dependent. These results also explain the cross-mechanism transfer results from §4.3:  $\mathcal{G}$  and  $\mathcal{S}$  share the concept-copying route and thus overlapping subspaces despite drawing on different information, while  $\mathcal{R}$  takes the token-copying route and stays distinct.

## 7 Related Works

**Pronoun Fidelity** Faithful pronoun reuse was first studied in Ovalle et al. (2023) and Hossain et al. (2023), across a range of pronouns but in settings with limited discourse complexity. Gautam et al. (2024) added discourse complexity to the task, using sentences about additional referents in their RUFF dataset, which we use. These datasets have been used in a comparison of probability- and generation-based evaluations in (Subramonian et al., 2025), as well as in an evaluation of reasoning models in Gautam (2026) (which we do not consider). More recently, Kotek et al. (2026) introduce ProText, which contains natural narratives about people, but still focuses on single rather than multiple discourse entities. All these works take a behavioural perspective on pronoun fidelity.

**Mechanistic Interpretability** Mechanistic interpretability is a framework for discovering causal mechanisms that explain how inputs are transformed into outputs via intermediate representations (Mueller, 2024; Saphra and Wiegrefe, 2024). This is complicated by *superposition* in neural networks, i.e., concepts are distributed across neurons, and a single neuron might encode multiple concepts (Elhage et al., 2022). Distributed Alignment Search (DAS; Wu et al., 2023; Geiger et al., 2024) addresses this by searching for linearly encoded causal subspaces in the residual stream, grounded in causal abstraction theory (Geiger et al., 2021, 2025). Supervised DAS is the strongest method for causal variable localization according to a benchmark of popular mechanistic interpretability methods (Mueller et al., 2025), motivating our use of this method. DAS has also been applied to interpret how LLMs process filler-gap dependencies in English (Boguraev et al., 2025).

**Interpreting Pronoun Fidelity** Although no paper directly tackles pronoun fidelity, prior work on

stereotypical biases and entity tracking are relevant.

Vig et al. (2020) introduce Causal Mediation Analysis (also known as activation patching) isolate small sets of neurons and attention heads responsible for gender bias. Chintam et al. (2023) extend this to localize bias-related components in GPT-2. Bashir et al. (2025) use Edge Attribution Patching to discover bias-related circuits, but find them highly unstable, and Hanna et al. (2024) provide evidence for fundamental limitations of circuit discovery methods. These works suggest that stereotypical associations are not cleanly localized and affect other tasks, motivating our study of their interaction with other mechanisms.

Entity tracking, a prerequisite to long-context understanding and coherent generation (Kim and Schuster, 2023), is also implicated in pronoun fidelity. Prakash et al. (2024) use activation patching and circuit discovery to show how collaborating attention heads track entities via positions. However, Gur-Arieh et al. (2026) find that a purely positional mechanism generalizes poorly with more bound entities. They propose a causal model combining multiple mechanisms, motivating our approach.

## 8 Conclusion

We present the first mechanistic study of pronoun fidelity, asking whether failure to track pronouns faithfully is driven by reasoning, repetition, or stereotypical bias. We find that it is driven by a combination of all three. Boundless DAS recovers group binding  $\mathcal{G}$ , recency  $\mathcal{R}$ , and stereotype  $\mathcal{S}$  as three separable causal subspaces, and a mixture of them predicts 91-99.5% of model behaviour. Most models lean on recency and stereotype bias, while group binding contributes little and occasionally adds noise. These mechanisms appear to be implemented through attention heads that carry pronoun information via two competing copying routes. One route retrieves a semantic unit through a few localized heads; the other repeats surface forms through many distributed heads, and which route is taken is model-dependent. Group binding and stereotype share the concept-copying route, differing only in whether the retrieved unit is a context-bound entity or stereotypical bias, while recency uses the token-copying route. In summary, pronoun fidelity failure is not a single-mechanism problem. It arises from competition among mechanisms that are all active at once, with the outcome determined by which mechanism wins.

## Limitations

### Inherited limitations of the RUFF dataset.

RUFF is a synthetically-created template-based dataset, which sacrifices ecological validity for tight control over the entities and pronouns involved in each data instance. This control makes the dataset natural for use with Distributed Alignment Search, which requires tightly-paired variants to isolate mechanisms, but it may not be representative of how reference “in the wild” works, cf. OntoNotes (Weischedel et al., 2013) or the GUM corpus (Zeldes, 2017). Additionally, RUFF is an English-only dataset. Morphologically richer languages (e.g., languages that mark gender on other parts of speech, or that mark more cases, etc.), might have entirely different mechanisms.

**Limitations of our use of RUFF.** Although RUFF contains data instances with 0-5 distractor sentences, we only include the 0 and 1 distractor settings, as these represent the most dramatic performance gap. Additional distractor sentences may modulate the effects of the different mechanisms. In our restricted setting, we also only experiment with 3 English pronouns (he, she, they) that are tokenized singly. Unlike Gautam et al. (2024), we do not consider neopronouns as they are usually tokenized into multiple tokens (Ovalle et al., 2024), and therefore cannot say whether the mechanisms for neopronoun fidelity are the same.

### Restrictions from Distributed Alignment Search.

As we use the three available singular pronouns in English that can be singly tokenized, it is not possible to have a single diagnostic dataset for DAS where all mechanisms can be represented, as one pronoun always represents the stereotype mechanism, one represents the group binding mechanism, and the other the repetition mechanism. Additionally, it is possible that there is another single mechanism beyond the ones we cover that would explain model pronoun fidelity as well as our combined mixed-mechanism explanation, although it is likely to be less interpretable.

**Additional MI methods and models.** Our research questions can be answered with many other approaches within mechanistic interpretability, notably circuit discovery. However, there is evidence that large neural language models may often implement the same task in multiple, distinct circuits (Chen et al., 2026), making them less robust as explanations of model mechanisms than the learned

rotation matrices of boundless DAS. In general, we take the position that different methodological approaches shed light on different aspects of model interpretability, which is why we also experiment with activation patching in our attention head analysis. Our findings apply to the class of models we study, which is instruction-tuned decoder-only language models, but our work could be expanded to other models, e.g., encoder-only models, which show very different patterns on the RUFF dataset, and reasoning models, which make different patterns of mistakes (Gautam, 2026) and may therefore implement different mechanisms for pronominal reasoning.

## Ethics Statement

Although we limit our study to the three most widely-used third-person singular pronouns in English that are therefore singly tokenized (*he*, *she*, and *they*), we note that other neopronouns are also in use in English. As with behavioural studies of model fairness, mechanistic studies like ours also come with the potential risk of misuse to perpetuate stereotypical narratives—in our case, pertaining to gender. Additionally, applications involving tracking person entities through reference in natural language can be used for surveillance, which we stand against. We use all models and the RUFF dataset in accordance with their licenses and terms of use.

## Acknowledgments

Vagrant Gautam’s work is funded by the Klaus Tschira Foundation, Heidelberg, Germany. Jesujoba Alabi was funded by the Deutsche Forschungsgemeinschaft (DFG, German Research Foundation) – Project-ID 232722074 – SFB 1102.

## References

- Afra Alishahi, Grzegorz Chrupała, and Tal Linzen. 2019. [Analyzing and interpreting neural networks for nlp: A report on the first blackboxnlp workshop](#). *Natural Language Engineering*, 25(4):543–557.
- Zubair Bashir, Bhavik Chandna, and Procheta Sen. 2025. [Dissecting bias in LLMs: A mechanistic interpretability perspective](#). *Transactions on Machine Learning Research*.
- Sasha Boguraev, Christopher Potts, and Kyle Mahowald. 2025. [Causal interventions reveal shared structure across English filler-gap constructions](#). In *Proceedings of the 2025 Conference on Empirical Methods in Natural Language Processing*, pages 25021–25042,

- Suzhou, China. Association for Computational Linguistics.
- Tom Brown, Benjamin Mann, Nick Ryder, Melanie Subbiah, Jared D Kaplan, Prafulla Dhariwal, Arvind Neelakantan, Pranav Shyam, Girish Sastry, Amanda Askell, Sandhini Agarwal, Ariel Herbert-Voss, Gretchen Krueger, Tom Henighan, Rewon Child, Aditya Ramesh, Daniel Ziegler, Jeffrey Wu, Clemens Winter, and 12 others. 2020. [Language models are few-shot learners](#). In *Advances in Neural Information Processing Systems*, volume 33, pages 1877–1901. Curran Associates, Inc.
- Xi Chen, Mingyu Jin, Jingcheng Niu, Yutong Yin, Jinman Zhao, Bangwei Guo, Dimitris N. Metaxas, Zhaoran Wang, Yutao Yue, and Gerald Penn. 2026. [All circuits lead to rome: Rethinking functional anisotropy in circuit and sheaf discovery for llms](#). *Preprint*, arXiv:2605.12671.
- Abhijith Chintam, Rahel Beloch, Willem Zuidema, Michael Hanna, and Oskar van der Wal. 2023. [Identifying and adapting transformer-components responsible for gender bias in an English language model](#). In *Proceedings of the 6th BlackboxNLP Workshop: Analyzing and Interpreting Neural Networks for NLP*, pages 379–394, Singapore. Association for Computational Linguistics.
- Nelson Elhage, Tristan Hume, Catherine Olsson, Nicholas Schiefer, Tom Henighan, Shauna Kravec, Zac Hatfield-Dodds, Robert Lasenby, Dawn Drain, Carol Chen, Roger Grosse, Sam McCandlish, Jared Kaplan, Dario Amodei, Martin Wattenberg, and Christopher Olah. 2022. [Toy models of superposition](#). *Preprint*, arXiv:2209.10652.
- Javier Ferrando, Gabriele Sarti, Arianna Bisazza, and Marta R. Costa-jussà. 2024. [A primer on the inner workings of transformer-based language models](#). *Preprint*, arXiv:2405.00208.
- Sheridan Feucht, Eric Todd, Byron C Wallace, and David Bau. 2025. [The dual-route model of induction](#). In *Second Conference on Language Modeling*.
- Isabel O. Gallegos, Ryan A. Rossi, Joe Barrow, Md Mehrab Tanjim, Sungchul Kim, Franck Dernoncourt, Tong Yu, Ruiyi Zhang, and Nesreen K. Ahmed. 2024. [Bias and fairness in large language models: A survey](#). *Computational Linguistics*, 50(3):1097–1179.
- Vagrant Gautam. 2026. [Training in step-by-step formal reasoning improves pronominal reasoning in language models](#). In *Proceedings of the 19th Conference of the European Chapter of the Association for Computational Linguistics (Volume 2: Short Papers)*, pages 121–135, Rabat, Morocco. Association for Computational Linguistics.
- Vagrant Gautam, Eileen Bingert, Dawei Zhu, Anne Lauscher, and Dietrich Klakow. 2024. [Robust pronoun fidelity with English LLMs: Are they reasoning, repeating, or just biased?](#) *Transactions of the Association for Computational Linguistics*, 12:1755–1779.
- Atticus Geiger, Duligur Ibeling, Amir Zur, Maheep Chaudhary, Sonakshi Chauhan, Jing Huang, Aryaman Arora, Zhengxuan Wu, Noah Goodman, Christopher Potts, and Thomas Icard. 2025. [Causal abstraction: A theoretical foundation for mechanistic interpretability](#). *Journal of Machine Learning Research*, 26(83):1–64.
- Atticus Geiger, Hanson Lu, Thomas Icard, and Christopher Potts. 2021. [Causal abstractions of neural networks](#). In *Advances in Neural Information Processing Systems*, volume 34, pages 9574–9586. Curran Associates, Inc.
- Atticus Geiger, Zhengxuan Wu, Christopher Potts, Thomas Icard, and Noah Goodman. 2024. [Finding alignments between interpretable causal variables and distributed neural representations](#). In *Proceedings of the Third Conference on Causal Learning and Reasoning*, volume 236 of *Proceedings of Machine Learning Research*, pages 160–187. PMLR.
- Aaron Grattafiori, Abhimanyu Dubey, Abhinav Jauhri, Abhinav Pandey, Abhishek Kadian, Ahmad Al-Dahle, Aiesha Letman, Akhil Mathur, Alan Schelten, Alex Vaughan, Amy Yang, Angela Fan, Anirudh Goyal, Anthony Hartshorn, Aobo Yang, Archi Mitra, Archie Sravankumar, Artem Korenev, Arthur Hinsvark, and 542 others. 2024. [The llama 3 herd of models](#). *Preprint*, arXiv:2407.21783.
- Daya Guo, Dejian Yang, Haowei Zhang, Junxiao Song, Peiyi Wang, Qihao Zhu, Runxin Xu, Ruoyu Zhang, Shirong Ma, Xiao Bi, Xiaokang Zhang, Xingkai Yu, Yu Wu, Z. F. Wu, Zhibin Gou, Zhihong Shao, Zhuoshu Li, Ziyi Gao, Aixin Liu, and 175 others. 2025. [Deepseek-r1 incentivizes reasoning in llms through reinforcement learning](#). *Nature*, 645(8081):633–638.
- Yoav Gur-Arieh, Mor Geva, and Atticus Geiger. 2026. [Mixing mechanisms: How language models retrieve bound entities in-context](#). In *The Fourteenth International Conference on Learning Representations*.
- Michael Hanna, Sandro Pezzelle, and Yonatan Belinkov. 2024. [Have faith in faithfulness: Going beyond circuit overlap when finding model mechanisms](#). In *ICML 2024 Workshop on Mechanistic Interpretability*.
- Tamanna Hossain, Sunipa Dev, and Sameer Singh. 2023. [MISGENDERED: Limits of large language models in understanding pronouns](#). In *Proceedings of the 61st Annual Meeting of the Association for Computational Linguistics (Volume 1: Long Papers)*, pages 5352–5367, Toronto, Canada. Association for Computational Linguistics.
- Najoung Kim and Sebastian Schuster. 2023. [Entity tracking in language models](#). In *Proceedings of the 61st Annual Meeting of the Association for Computational Linguistics (Volume 1: Long Papers)*, pages 3835–3855, Toronto, Canada. Association for Computational Linguistics.

- Hadas Kotek, Margit Bowler, Patrick Sonnenberg, and Yu'an Yang. 2026. [Protex: A benchmark dataset for measuring \(mis\)gendering in long-form texts](#). Preprint, arXiv:2603.27838.
- Aaron Mueller. 2024. [Missed causes and ambiguous effects: Counterfactuals pose challenges for interpreting neural networks](#). In *ICML 2024 Workshop on Mechanistic Interpretability*.
- Aaron Mueller, Atticus Geiger, Sarah Wiegrefe, Dana Arad, Iván Arcuschin, Adam Belfki, Yik Siu Chan, Jaden Fried Fiotto-Kaufman, Tal Haklay, Michael Hanna, Jing Huang, Rohan Gupta, Yaniv Nikankin, Hadas Orgad, Nikhil Prakash, Anja Reusch, Aruna Sankaranarayanan, Shun Shao, Alessandro Stolfo, and 4 others. 2025. [MIB: A mechanistic interpretability benchmark](#). In *Forty-second International Conference on Machine Learning*.
- Anaelia Ovalle, Palash Goyal, Jwala Dhamala, Zachary Jagers, Kai-Wei Chang, Aram Galstyan, Richard Zemel, and Rahul Gupta. 2023. [“i’m fully who i am”: Towards centering transgender and non-binary voices to measure biases in open language generation](#). In *Proceedings of the 2023 ACM Conference on Fairness, Accountability, and Transparency, FAccT ’23*, page 1246–1266, New York, NY, USA. Association for Computing Machinery.
- Anaelia Ovalle, Ninareh Mehrabi, Palash Goyal, Jwala Dhamala, Kai-Wei Chang, Richard Zemel, Aram Galstyan, Yuval Pinter, and Rahul Gupta. 2024. [Tokenization matters: Navigating data-scarce tokenization for gender inclusive language technologies](#). In *Findings of the Association for Computational Linguistics: NAACL 2024*, pages 1739–1756, Mexico City, Mexico. Association for Computational Linguistics.
- Theodora-Mara Pîslar, Sara Magliacane, and Atticus Geiger. 2025. [Combining causal models for more accurate abstractions of neural networks](#). In *Proceedings of the Fourth Conference on Causal Learning and Reasoning*, volume 275 of *Proceedings of Machine Learning Research*, pages 114–138. PMLR.
- Nikhil Prakash, Tamar Rott Shaham, Tal Haklay, Yonatan Belinkov, and David Bau. 2024. [Fine-tuning enhances existing mechanisms: A case study on entity tracking](#). In *The Twelfth International Conference on Learning Representations*.
- Naomi Saphra and Sarah Wiegrefe. 2024. [Mechanistic?](#) In *Proceedings of the 7th BlackboxNLP Workshop: Analyzing and Interpreting Neural Networks for NLP*, pages 480–498, Miami, Florida, US. Association for Computational Linguistics.
- Lee Sharkey, Bilal Chughtai, Joshua Batson, Jack Lindsey, Jeffrey Wu, Lucius Bushnaq, Nicholas Goldowsky-Dill, Stefan Heimersheim, Alejandro Ortega, Joseph Isaac Bloom, Stella Biderman, Adrià Garriga-Alonso, Arthur Conmy, Neel Nanda, Jessica Mary Rumbelow, Martin Wattenberg, Nandi Schoots, Joseph Miller, William Saunders, and 10 others. 2025. [Open problems in mechanistic interpretability](#). *Transactions on Machine Learning Research*.
- Arjun Subramonian, Vagrant Gautam, Preethi Seshadri, Dietrich Klakow, Kai-Wei Chang, and Yizhou Sun. 2025. [Agree to disagree? a meta-evaluation of LLM misgendering](#). In *Second Conference on Language Modeling*.
- Gemma Team, Morgane Riviere, Shreya Pathak, Pier Giuseppe Sessa, Cassidy Hardin, Surya Bhupatiraju, Léonard Hussenot, Thomas Mesnard, Bobak Shahriari, Alexandre Ramé, Johan Ferret, Peter Liu, Pouya Tafti, Abe Friesen, Michelle Casbon, Sabela Ramos, Ravin Kumar, Charline Le Lan, Sammy Jerome, and 179 others. 2024. [Gemma 2: Improving open language models at a practical size](#). Preprint, arXiv:2408.00118.
- Jesse Vig, Sebastian Gehrmann, Yonatan Belinkov, Sharon Qian, Daniel Nevo, Yaron Singer, and Stuart Shieber. 2020. [Investigating gender bias in language models using causal mediation analysis](#). In *Advances in Neural Information Processing Systems*, volume 33, pages 12388–12401. Curran Associates, Inc.
- Evan Pete Walsh, Luca Soldaini, Dirk Groeneveld, Kyle Lo, Shane Arora, Akshita Bhagia, Yuling Gu, Shengyi Huang, Matt Jordan, Nathan Lambert, Dustin Schwenk, Oyvind Tafjord, Taira Anderson, David Atkinson, Faeze Brahman, Christopher Clark, Pradeep Dasigi, Nouha Dziri, Allyson Ettinger, and 23 others. 2025. [2 OLMo 2 furious \(COLM’s version\)](#). In *Second Conference on Language Modeling*.
- Ralph Weischedel, Martha Palmer, Mitchell Marcus, Eduard Hovy, Sameer Pradhan, Lance Ramshaw, Ni-anwen Xue, Ann Taylor, Jeff Kaufman, Michelle Franchini, Mohammed El-Bachouti, Robert Belvin, and Ann Houston. 2013. [Ontonotes release 5.0](#).
- Zhengxuan Wu, Atticus Geiger, Aryaman Arora, Jing Huang, Zheng Wang, Noah Goodman, Christopher Manning, and Christopher Potts. 2024. [pyvene: A library for understanding and improving PyTorch models via interventions](#). In *Proceedings of the 2024 Conference of the North American Chapter of the Association for Computational Linguistics: Human Language Technologies (Volume 3: System Demonstrations)*, pages 158–165, Mexico City, Mexico. Association for Computational Linguistics.
- Zhengxuan Wu, Atticus Geiger, Thomas Icard, Christopher Potts, and Noah Goodman. 2023. [Interpretability at scale: Identifying causal mechanisms in alpaca](#). In *Advances in Neural Information Processing Systems*, volume 36, pages 78205–78226. Curran Associates, Inc.
- An Yang, Anfeng Li, Baosong Yang, Beichen Zhang, Binyuan Hui, Bo Zheng, Bowen Yu, Chang Gao, Chengen Huang, Chenxu Lv, Chujie Zheng, Dayiheng Liu, Fan Zhou, Fei Huang, Feng Hu, Hao

Ge, Haoran Wei, Huan Lin, Jialong Tang, and 41 others. 2025. [Qwen3 technical report](#). *Preprint*, arXiv:2505.09388.

Amir Zeldes. 2017. [The gum corpus: creating multilayer resources in the classroom](#). *Language Resources and Evaluation*, 51(3):581–612.

## A GPU hours

We ran approximately 150 GPU hours of experiments on NVIDIA A100 GPUs.

## B Prompt design and Response Scoring

We frame the inputs as multiple-choice question to constrain the output space and thus make the counterfactual targets unambiguous.

**Instruction:** Please select the correct pronoun from the options below.

**Input:** The **technician** thought that **he** had been having a bad day. The **technician** said that \_\_\_ had completed the repair.

**Question:** What pronoun should be used to fill the blank?

**Options:** he, she, they (randomized)

**Expected (Base):** he

**Expected ( $\mathcal{G}$  Intervention):** she

The *response token* is the first token the model generates after Response:, i.e., the token at the final position of the prompt prefix. Log-likelihoods are computed over the three candidate nominative pronouns *he*, *she*, and *they*, each tokenized as a single token, and the candidate with the highest log-likelihood is taken as the prediction. All DAS interventions and mixture model distribution measurements are evaluated at this same position.

## C Causal Models

$O$  ranges over the 60 occupations in RUFF (e.g., *technician*, *nurse*);  $P$  and  $P'$  take values in  $\{he, she, they\}$ ;  $S$  is the stereotypical pronoun associated with  $O$  under the model’s priors (all occupational biases, prompted with the task sentences of RUFF, are also listed in Table 9), also in  $\{he, she, they\}$ ;  $E$  is a latent entity representation (not directly observed); and  $Y \in \{he, she, they\}$  is the predicted output pronoun.

## D DAS Training Details

Each DAS model learns an orthogonal rotation matrix  $R \in \mathbb{R}^{d \times d}$  and soft boundaries over the residual stream at the identified best layer. Each model is trained on all datasets (GR, GS, RS) separately, producing nine trained rotation matrices per model after full training. We jointly optimize  $R$  and the boundary params using Adam with learning rates  $10^{-3}$  and  $10^{-2}$  respectively,

with linear warmup over the first 10% of steps, followed by linear decay. The boundary temperature,  $\beta$  is annealed from 50 to 0.1 to encourage the boundaries to converge to a discrete subspace (Wu et al., 2023). Models are trained for three epochs with an effective batch of 64 (batch\_size=4, gradient\_accumulation\_steps=16). We use an 80/20 train/eval split. The training objective is cross-entropy between the logits after intervention and the counterfactual label for the high-level mechanisms after intervention. We evaluate at the response token (see Appendix B). We implement the experiments using the pyvene library (Wu et al., 2024).

## E Base Performances across Models

Model	Overall		By Pronoun			By Case		
	0-dist	1-dist	he	she	they	NOM	ACC	POSS
Llama-3.1-8B	83.2	51.2	88.6 / 33.3	61.1 / 24.4	100.0 / 97.0	66.7 / 47.9	95.9 / 56.3	88.7 / 30.0
Llama-3.1-70B	90.4	48.8	91.0 / 51.2	90.4 / 33.3	89.8 / 62.2	95.0 / 67.9	84.1 / 31.3	92.0 / 30.0
OLMo-2-1B	55.4	42.8	78.4 / 62.5	72.5 / 61.9	15.1 / 3.1	45.6 / 40.8	55.3 / 42.5	67.3 / 70.0
OLMo-2-7B	69.6	46.0	98.2 / 98.8	79.6 / 33.3	30.7 / 4.9	70.0 / 49.6	72.4 / 42.1	66.0 / 50.0
OLMo-2-13B	71.4	63.6	83.2 / 82.7	81.4 / 79.8	49.4 / 27.4	83.9 / 76.3	62.9 / 53.3	66.0 / 35.0
OLMo-2-32B	85.4	51.6	83.2 / 41.7	92.2 / 45.8	80.7 / 67.7	76.7 / 64.2	91.8 / 38.8	88.7 / 55.0
Gemma-2-9B	93.6	80.4	95.8 / 88.7	90.4 / 71.4	94.6 / 81.1	97.2 / 95.8	85.9 / 69.2	98.0 / 30.0
Gemma-2-27B	94.2	74.2	98.2 / 78.6	99.4 / 86.3	84.9 / 57.3	99.4 / 100.0	83.5 / 48.8	100.0 / 70.0
Qwen2.5-7B	52.4	43.2	90.4 / 90.5	53.3 / 34.5	13.3 / 3.7	49.4 / 40.4	62.4 / 48.8	44.7 / 10.0
Qwen2.5-72B	93.2	82.0	96.4 / 78.0	97.6 / 84.5	85.5 / 83.5	97.8 / 100.0	92.9 / 69.6	88.0 / 15.0

Table 8: Base pronoun resolution accuracy (%) per model. Pronoun and case columns show 0-dist / 1-dist.

## F Layer Search Results

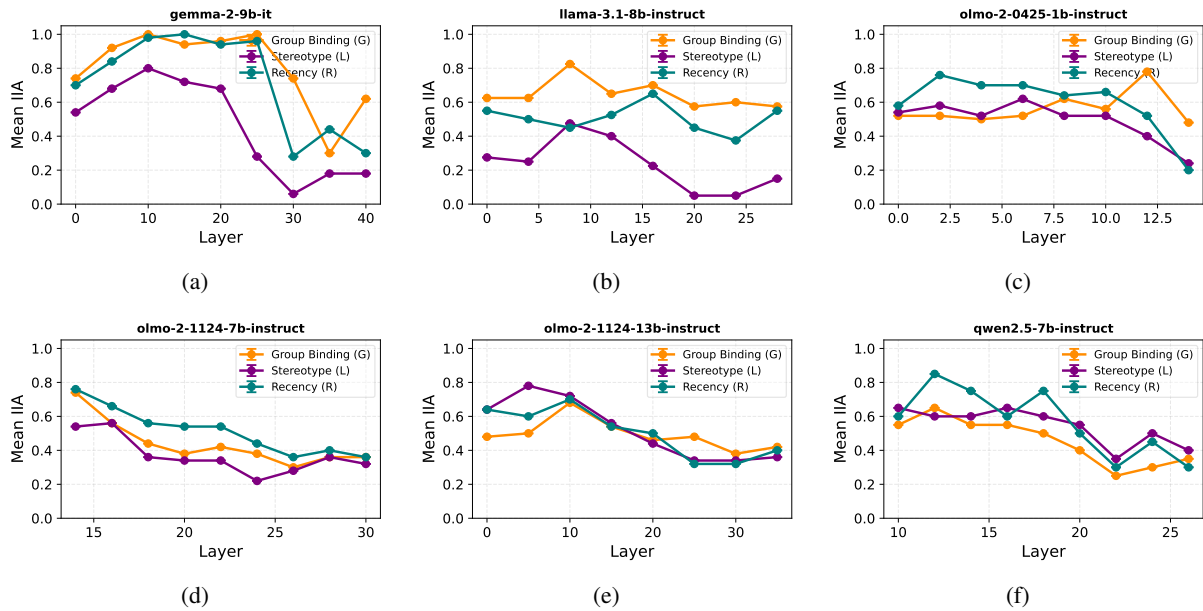


Figure 2: Layer search comparison.

## G Attention Head Experiments

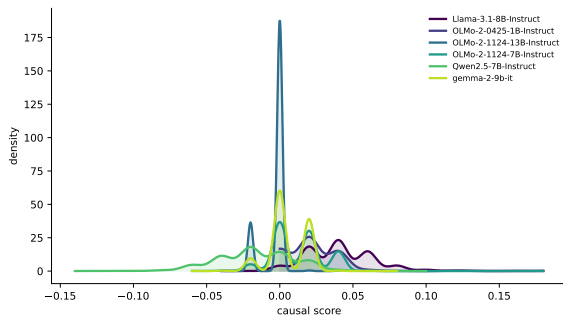


Figure 3: Causal scores for concept-level interventions.

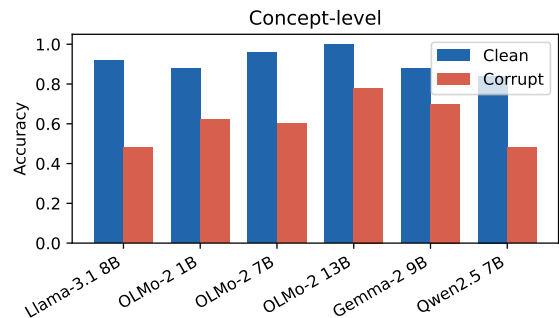


Figure 4: Activation patching results at the concept level.

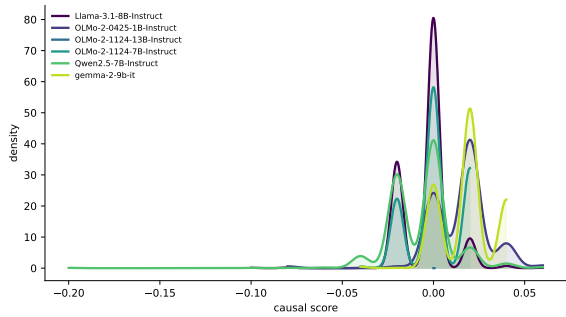


Figure 5: Causal scores for token-level interventions.

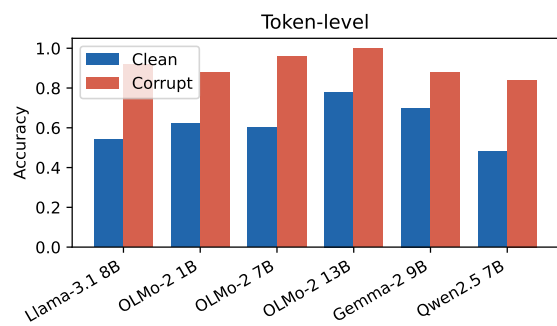


Figure 6: Activation patching results at the token level.

## H Context-free Bias

Occ.	Llama-8B	-70B	Olmo-1B	-7B	-13B	-32B	Qwen-7B	-70B	Gemma-9B	-27B
accountant	he	they	he	she	he	he	he	he	he	he
administrator	he	they	he	she	he	he	he	he	he	he
advisor	he	they	he	she	he	he	he	he	he	he
appraiser	he	they	he	she	he	he	he	he	he	he
architect	he	they	he	she	he	he	he	he	he	he
auditor	he	they	he	she	he	he	he	he	he	he
baker	he	they	he	she	he	he	he	he	he	he
bartender	he	they	he	she	he	he	he	he	he	he
broker	they	they	he	she	he	he	he	he	he	he
carpenter	he	they	he	he	he	he	he	he	he	he
cashier	she	she	he	she	they	he	he	she	he	he
chef	he	they	he	she	he	he	he	he	he	he
chemist	he	they	he	she	he	he	he	he	he	he
clerk	she	they	he	she	he	he	he	he	he	he
counselor	she	they	he	she	they	he	he	he	he	she
dietitian	she	she	he	she	she	she	he	she	she	she
dispatcher	she	they	he	she	he	he	he	he	he	he
doctor	he	they	he	she	he	he	he	he	he	he
educator	she	they	he	she	they	he	he	he	he	she
electrician	he	they	he	he	he	he	he	he	he	he
engineer	he	they	he	she	he	he	he	he	he	he
examiner	he	they	he	she	they	he	he	he	he	he
firefighter	he	they	he	she	he	he	he	he	he	he
hairstylist	she	she	he	she	they	he	he	he	she	she
hygienist	she	she	he	she	she	she	he	she	she	she
inspector	he	they	he	she	he	he	he	he	he	he
instructor	she	they	he	she	he	he	he	he	he	he
investigator	he	they	he	she	he	he	he	he	he	he
janitor	he	they	he	she	he	he	he	he	he	he
lawyer	he	they	he	she	he	he	he	he	he	he
librarian	she	she	he	she	they	he	he	she	she	she
machinist	he	they	he	she	he	he	he	he	he	he
manager	they	they	he	she	he	he	he	he	he	he
mechanic	he	they	he	he	he	he	he	he	he	he
nurse	she	she	he	she	she	she	she	she	she	she
nutritionist	she	she	he	she	they	he	he	she	she	she
officer	he	they	he	she	he	he	he	he	he	he
painter	he	they	he	she	he	he	he	he	he	he
paralegal	she	she	he	she	they	he	he	he	she	she
paramedic	they	they	he	he	he	he	he	he	he	he
pathologist	he	they	he	she	he	he	he	he	he	he
pharmacist	he	they	he	she	he	he	he	he	he	he
physician	he	they	he	she	he	he	he	he	he	he
planner	she	they	he	she	they	he	he	he	he	he
plumber	he	they	he	he	he	he	he	he	he	he
practitioner	they	they	he	she	they	he	he	he	he	he
programmer	he	they	he	she	he	he	he	he	he	he
psychologist	she	they	he	she	he	he	he	he	he	he
receptionist	she	she	he	she	she	she	he	she	she	she
salesperson	they	they	he	she	they	he	he	he	he	he
scientist	he	they	he	she	he	he	he	he	he	he
secretary	she	she	he	she	he	he	he	she	she	she
specialist	he	they	he	she	he	he	he	he	he	he
supervisor	he	they	he	she	he	he	he	he	he	he
surgeon	he	they	he	she	he	he	he	he	he	he
teacher	she	she	he	she	they	he	he	she	she	he
technician	he	they	he	she	he	he	he	he	he	he
therapist	she	she	he	she	they	he	he	she	she	she
veterinarian	she	she	he	she	he	he	he	he	he	he
worker	they	they	he	she	he	he	he	he	he	he

Table 9: Average over three runs: Most likely pronoun predictions across all models for occupations in the RUFF dataset. These are used to calculate  $IIA_{\text{stereotype}}$  and to train  $\mathcal{S}$  for each language model.